DOI: 10.1002/ejic.200601113

Unusual Magnetic Behavior of a 2D Citrate-Bridged Dysprosium(III) Coordination Polymer

Feng-Yan Li,[a] Lin Xu,*[a] Guang-Gang Gao,[a] Li-Hua Fan,[a] and Bo Bi[a]

Keywords: Lanthanides / Coordination chemistry / Magnetic properties / Hydrothermal synthesis

A new lanthanide citrate coordination polymer [Dy(citrate)-$(H_2O)]_n$ (**1**) was hydrothermally synthesized and structurally characterized by elemental analyses, single-crystal X-ray diffraction, IR spectroscopy, thermogravimetric analysis, photoluminescence spectrum, and magnetic measurements. The structure of **1** exhibits a 2D layer structure, in which the Dy_2O_2 dimer serves as the building block. The photoluminescence spectrum shows blue luminescence in the solid state at room temperature. Owing to the special frustration structure, unusual magnetic relaxation was found in compound **1**.

Introduction

The current interest in the synthesis of new metal–organic coordination polymers continues to expand in virtue of not only their intriguing variety of architectures, but also their potential applications in many fields, such as catalysis, material science, medicine, and magnetochemistry,[1–4] which may originate either from the metal centers and/or the organic components. Recently, polycarboxylates have been widely used to produce high-nuclearity magnetic clusters.[5–8] Particularly attractive interest is the construction of lanthanide carboxylates, owing to the wide variety of structures and their unique f–f electronic transitions.

Citric acid, a hydroxy tricarboxylic acid, is well known on account of its important role in biosystems. Moreover, it was found to be a versatile ligand in coordination chemistry by virtue of its conformational flexibility, its ability to deprotonate completely or partially, and its diversity in complexing behavior. A large number of metal–citrate compounds have been structurally characterized.[5–11] However, most of the work in this area has focused on the assembly of the d-block metals. By contrast, less work has been done to date on the lanthanide–citrate systems.[12] Additionally, the reported work of the lanthanide–citrates mostly concentrates on their luminescent properties, whereas the rich magnetic properties of lanthanide–citrate have been neglected. To the best of our knowledge, there has been only one reported lanthanide–citrate polymer that was studied with its magnetic properties, in which ferromagnetic exchange interactions were found between the neighboring magnetic centers.[12d] Hence, the citrate ligand could act as an efficient magnetic coupler owing to its diverse bridging modes.

It is well known that in the f-block the Dy compounds generally exhibit novel magnetic properties as well as the Gd, Tb, Ho, and Er complexes. In the Dy cluster compounds reported in the literature, most of them display frequency-dependent, out-of-phase AC signals, magnetization hysteresis loops, or quantum tunneling behavior, such as the triangular dysprosium compound $[Dy_3(\mu_3\text{-}OH)_2L_3Cl_2(H_2O)_4]$ $[Dy_3(\mu_3\text{-}OH)_2L_3Cl(H_2O)_5]Cl_5\cdot 19H_2O$ (HL = *o*-vanillin),[13a] and the dysprosium–manganese cluster $[Dy_6Mn_6(Hshi)_2(shi)_{10}(CH_3OH)_{10}(H_2O)_2]\cdot 9CH_3OH\cdot 8H_2O$ (H_3shi = salicylhydroxamic acid).[13b] Also, in the complex $[Mn_{11}Dy_4O_8(OH)_6(OMe)_2(O_2CPh)_{16}(NO_3)_5(H_2O)_3]\cdot$ 15MeCN, magnetization hysteresis loops and quantum tunneling behavior have been observed.[13c] Noting that dysprosium(III) shows manifold magnetic behavior and the aforementioned features of the citrate, we decided to explore the assembly of the Dy–citrate polymer and investigate its magnetic properties, aiming to obtain new compounds with novel magnetic properties.

In this paper, by using hydrothermal synthesis, which has become a convenient technique for the preparation of a wide range of organic–inorganic hybrid materials, we successfully prepared a lanthanide citrate complex: [Dy-(citrate)$(H_2O)]_n$, which exhibits a 2D layer structure, in which the Dy_2O_2 dimer serves as the building block. Weak antiferromagnetic interactions were found between the Dy ions in the layer. With an applied magnetic field, unusual magnetic relaxation was observed owing to the frustration structure.

[a] Key Laboratory of Polyoxometalates, Science of Ministry of Education, College of Chemistry, Northeast Normal University,
Changchun, 130024 P. R. China
E-mail: linxu@nenu.edu.cn
Supporting information for this article is available on the WWW under http://www.eurjic.org or from the author.

Results and Discussion

Description of the Crystal Structure

Single-crystal X-ray analysis revealed that complex **1** crystallizes in the monoclinic space group *C*2/*c*. In compound **1**, there is one crystallographically independent Dy^{III} ion. The Dy ion has a nine-coordinate environment, seven of which are occupied by seven carboxylate oxygen atoms from four citrate ions, and the other two sites are occupied by one hydroxy oxygen of the citrate ion and one water molecule oxygen. The O4 and O8 atoms from one β-carboxylate are bonded in a chelated mode. Also, the ligand has a tridentate coordination mode and binds through one *α*-carboxylate (O3), one β-carboxylate (O7), and the *α*-hydroxy (O1) oxygen atoms (see Figure 1). The adjacent Dy^{III} ions are edge-shared through O(7) and O($7^{\#2}$), resulting in the formation of a Dy_2O_2 dimer (see Figure S1); the dinuclear Dy_2O_2 units are firstly linked by the central carboxylate of the citrate to form a ladder chain, and then the ladder chains are additionally bridged into a 2D layer structure by the terminal carboxylate of the citrate (see Figure 2). The adjacent layers are parallel and stack along the *c* axis without interpenetration, leading to a 3D framework by the H-bond interactions. (Figures S2 and S3).

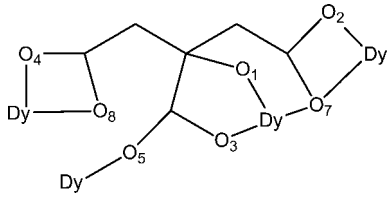

Figure 1. Structure of compound **1**.

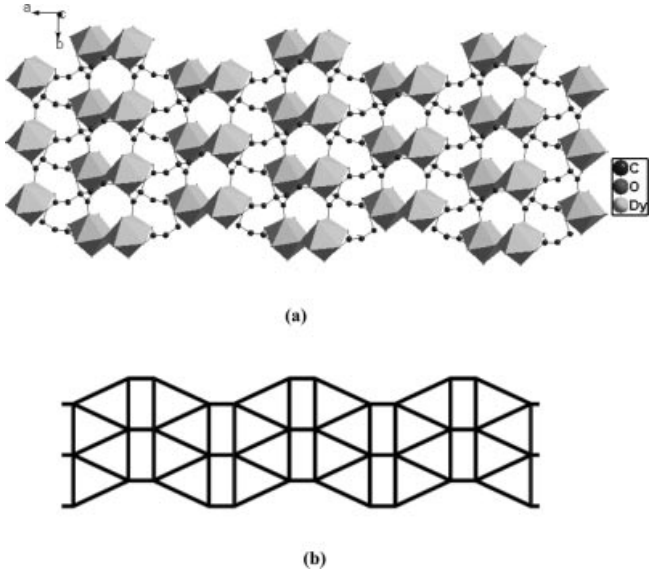

Figure 2. (a) 2D layer structure of compound **1** (viewed along the *c* axis). (b) A schematic illustration of the 2D layer structure.

Among the reported Ln–citrate series, $[Ln(Hcit)(H_2O)]_n$, Ln = La,[12a] Nd,[12b] the chains are bound together by covalent bonds with the citrate ligands, leading to 3D structures. When Ln = Gd, Nd,[12d] and with a relatively low temperature (100 °C) hydrothermal reaction, 1D chain structures are obtained. Whereas when Ln = Dy (this work), Eu, and Tb,[12c] 2D structure coordination polymers are formed. The versatile structures owe to the high coordination number of lanthanide ions and the flexible coordination geometry of citrate ligands.

In compound **1**, each Dy^{III} is coordinated to three symmetry-related citrate ligands whereas each citrate ion is coordinated to four Dy^{III} ions. The Dy–O bond lengths are in the range 2.321(2)–2.608(3) Å with an average of 2.423 Å and the closest distance between two neighboring Dy ions [bridged by μ_2-O(7)] is 4.104 Å (see Figure S1), which is shorter than that in $[Eu(citrate)(H_2O)]_n$[12c] (Eu–Eu: 4.162 Å) and $[Gd(Hcit)(H_2O)_2{\cdot}H_2O]$[12d] (Gd–Gd: 4.321 Å). Within the *ab* plane, square and triangle grids arrange alternately with Dy–Dy separations of 4.104, 6.076, and 6.619 Å (see Figure S4), which can be viewed as geometrically frustration system. Considering that the frustration structure will influence the orientation of the electron spin, we are interested with the magnetic behavior of compound **1**, and the magnetic study of compound **1** was carried out.

Magnetic Properties

Magnetic measurements were performed on a crystalline sample confined within a gelatin capsule under a field of 1 kOe in the temperature range 2–300 K. A plot of $\chi_m T$ vs. *T* is shown in Figure S5. The $\chi_m T$ value at room temperature is ca. 14.55 emu K mol^{-1} [closed to the expected value for one Dy^{3+} (S = 5/2, L = 5, $^6H_{15/2}$) of 14.18 emu K mol^{-1}], which decreases smoothly with decreasing temperature, reaching a minimum value of 13.45 emu K mol^{-1} at 12 K. With a further decrease in the temperature, $\chi_m T$ increases sharply, reaching a maximum value of 14.98 emu K mol^{-1}at 2.0 K. The thermal variation of $\chi_m T$ mainly depends on the populations of the Stark levels and on the possible antiferromagnetic or ferromagnetic interactions between the two Dy^{III} ions. It is well known that by interelectronic repulsion and spin-orbit coupling, the $4f^n$ configuration of a Ln^{III} ion is split into $^{2S+1}L_J$ states. The crystal-field perturbation further leads to the splitting into Stark components. At room temperature, all the Stark levels of the 16-fold degenerate $^6H_{15/2}$ ground states are populated. While the temperature decreases, a gradual depopulation of these levels takes place.[14a] Therefore, in order to elucidate the magnetic properties, the field dependence of the $\chi_m T$ product of **1** (Figure S6) was also measured in the range 2–30 K except for the data of thermal dependence at 1 kOe of the $\chi_m T$ product (Figure S5). When the field is less and equal to 10 kOe, the $\chi_m T$ value slightly increases below 5 K, suggesting the occurrence of a weak ferromagnetic interaction arising from Dy_2O_2 dimers (Figure S1). When the magnetic field is stronger than 20 kOe the $\chi_m T$ value decreases, which results from the field saturation effect. Because of the presence of the large unquenched orbital angular momentum and spin-orbit coupling, no satisfactory result of the fit is

obtained by introducing exchange interactions through a simple dimer law deduced from the isotropic spin Hamiltonian.

To investigate the magnetic properties in detail, the field dependence of the magnetization (0–50 kOe) for compound **1** was measured at 2, 5, 10, and 20 K (Figure 3). The magnetization at 2 and 5 K increases very rapidly in low field and reaches the saturation value of ca. 5.5 $N\beta$ at 50 kOe, whereas the magnetization at 10 and 20 K increases slowly as the magnetic field increases. Interestingly, a small hysteresis loop is observed at 2 K with a coercive field (H_c) of 10 Oe and remnant magnetization (M_r) of 94 Oe emu mol^{-1} (Figure 4), which is an intrinsic behavior, because a single-crystal sample was used in the measurements.

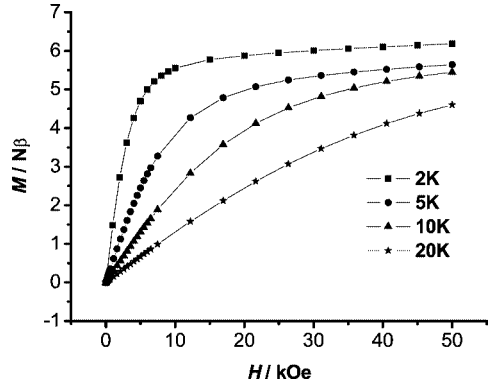

Figure 3. Magnetization vs. applied magnetic field plots at 2, 5, 10, and 20 K of complex **1**.

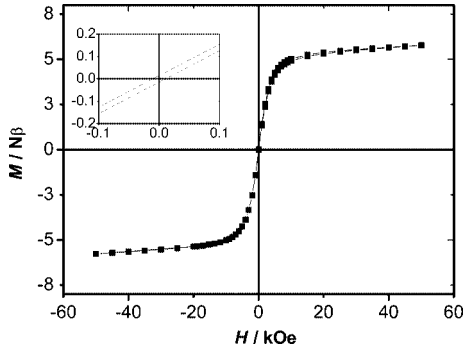

Figure 4. Hysteresis loop at 2 K for **1**. Inset: expansion showing the very small coercivity (left top).

The above unusual magnetic properties drive us to find sufficient reason for explanation. The temperature dependence of the alternating current magnetic susceptibility for compound **1** was thus measured in zero-dc field in the range of 2–20 K at different frequencies (1–1000 Hz) as shown in Figure 5. However, no frequency-dependent cusp was observed for either the in-phase component χ'_m or the out-of-phase component χ''_m at zero field, probably owing to weak coupling between Dy ions in **1** considering the long Dy···Dy separation. When a dc field (5 kOe) was applied, two peaks (T_p) appeared for both χ'_m and χ''_m, respectively (Figure 6), indicating a field-dependent magnetic behavior for compound **1**. Moreover, χ'_m and χ''_m are strongly frequency-dependent with a larger Φ value of 0.16 {$\Phi = (\Delta T_p/T_p)/[\Delta(\log f)]$} than that for normal spin glass (<0.1),[14b] displaying an unusual glass-like behavior. Such a result should be attributed to the geometrical frustration for Dy ions in compound **1**, because the 2D connection of the Dy ions in compound **1** appeared in the pattern of the alternately arrayed square and triangle grids (Figure 2b), which is similar to the Shastry–Sutherland lattice in compound DyB_4. The Shastry–Sutherland lattice was demonstrated to cause geometrical frustration in some magnetic systems.[15] Without the applied DC magnetic field, the magnetic interactions between the Dy ions in compound **1** are rather weak owing to the long Dy···Dy separations, which leads to the frustration unobserved. When the introduction of a DC field, the antiferromagnetic interaction between Dy ions could be enhanced and became dominant, leading to the unusual field-dependent magnetic relaxation behavior in compound **1**. Similar phenomenon was reported by Gao and co-workers.[16]

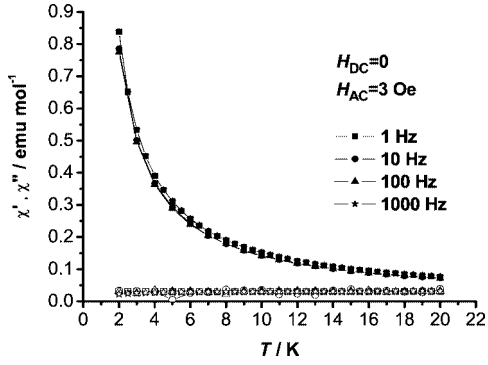

Figure 5. Temperature dependence of the real (top) and imaginary (bottom) components of the ac susceptibility in a zero applied static field with an oscillating field of 3 Oe at a frequency of 1–1000 Hz. The filled symbols are for the in-phase component χ'_m, the open symbols are for the out-of-phase component χ''_m.

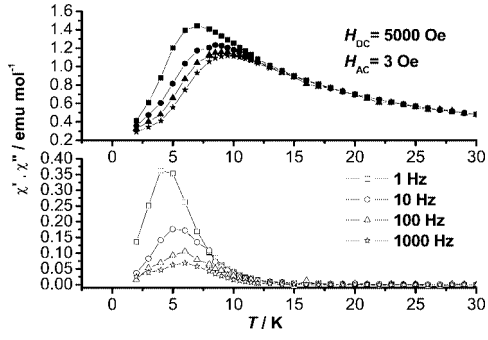

Figure 6. Frequency dependence of the AC susceptibility at 5 kOe applied static field with an oscillating field of 3 Oe at a frequency of 1–1000 Hz. The lines are guides.

IR Spectrum, Thermogravimetric Analysis (TGA), and Photoluminescence Properties

Strong characteristic absorptions around 1610, 1560, 1430, and 1380 cm^{-1} in the IR spectrum are observed for the carboxyl groups in compound **1**. No signal appears in

the region 1690 and 1730 cm^{-1}, indicating the complete deprotonation of the carboxyl groups in the complex. The TGA performed on **1** (as shown in Figure S7), shows that compound **1** is stable up to 250 °C, and the first weight loss in the range of 250–350 °C corresponds to the loss of coordinated water. The complete decomposition of **1** occurs at above 650 °C. The residual mass at 650 °C (55% approximately) corresponds to the formation of Dy_2O_3.

The photoluminescence spectrum of complex **1** is shown in Figure 7, which is blue luminescent in the solid state with typical Dy^{3+} emissions at 479, 570, and 620 nm that are ascribed to the characteristic emission $^4F_{9/2} \rightarrow {}^6H_J$ transitions of the Dy^{3+} ion (J = 15/2, 13/2, and 11/2). The strongest emission band is located at 479 nm ($^4F_{9/2} \rightarrow {}^6H_{15/2}$), suggesting the citric acid ligand is suitable for the sensitization of blue luminescence for Dy^{3+}.

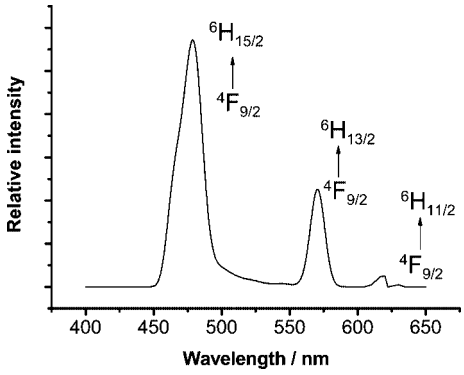

Figure 7. Emission spectra of compound **1** in the solid state at room temperature (excitation at 325 nm).

Conclusions

A new lanthanide 2D coordination polymer, in which the citrate bridges the Dy_2O_2 dimer into a 2D layer, was successfully produced by a hydrothermal reaction. The coordination polymer of dysprosium exhibits interesting magnetic properties in that the geometrical frustration resulting from the structure of the alternately arrayed square and triangle grids in compound **1** causes an unusual magnetic relaxation behavior, providing valuable information for exploring molecular magnetic materials with lanthanides.

Experimental Section

Materials and Methods: All purchased chemicals were of reagent grade and used without further purification. Elemental analyses (C, H, and N) were performed with a Perkin–Elmer 2400 Elemental Analyzer. Dy was determined by a Leaman inductively coupled plasma (ICP) spectrometer. The IR spectra were obtained in the range 400–4000 cm^{-1} with an Alpha Centaure FTIR spectrophotometer by using KBr pellets. Thermogravimetric analysis was performed with a Perkin–Elmer TGA7 instrument in flowing N_2 with a heating rate of 5 °C min^{-1}. The magnetic susceptibility measurements for **1** were carried out on polycrystalline samples by using a Quantum Design MPMS-XL-5 SQUID magnetometer in the temperature range 2–300 K and magnetic field up to 5 T. Diamagnetic corrections were estimated from Pascal's constants.

Synthesis: The title compound was hydrothermally synthesized [Equation (1)] under autogenous pressure. A mixture of Dy_2O_3 (0.1 g, 0.27 mmol), citric acid (0.192 g, 1.0 mmol), and water (10 mL) was simply stirred and then sealed in a 15-mL Teflon-lined autoclave, which was heated to 170 °C for 2 d. After slow cooling to room temperature at a rate of 10 °C h^{-1}, colorless block crystals of compound **1** were separated in pure phase (80% yield based on Dy). $C_6H_7DyO_8$ (369.59): calcd. C 19.49, H 1.89, Dy 43.98; found C 19.47, H 1.88, Dy 43.99. Compound **1** is insoluble in common organic solvent and water.

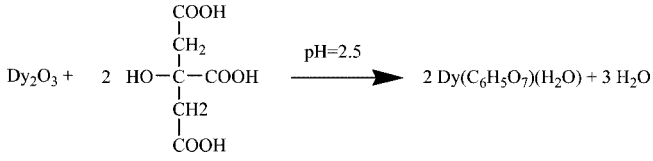

(1)

X-ray Crystallography: Crystal data for **1**: monoclinic, space group $C2/c$; a = 19.145(4), b = 6.076(12), c = 15.577(3) Å; β = 103.35(3)°; V = 1762.9(6) $Å^3$; T = 298 K; Z = 8; μ = 8.5 mm^{-1}; 8178 reflections measured, 2013 unique (R_{int} = 0.0269) which were used in all calculations. The structure was solved by direct methods by using the program SHELXS-97 and refined by full-matrix least-squares methods on F^2 with the use of the SHELXL-97 program package. Structure solution and refinement based on 2013 independent reflections with $I > 2\sigma(I)$ and 136 parameters gave $R_1(wR_2)$ = 0.0192 (0.0507). The structure of compound **1** was determined by single-crystal X-ray diffraction. A single colorless crystal with approximate dimensions of 0.2 × 0.1 × 0.1 mm was mounted to the end of a glass fiber capillary. Data were collected with a Rigaku R-AXIS RAPID IP diffractometer at 293 K by using graphite-monochromated Mo-K_α radiation (λ = 0.71073 Å) and oscillation scans technique in the range of $3.05 < \theta < 27.47°$. A summary of the crystal data and structure refinement for compound **1** is provided in Table 1. Selected bond lengths and bond angles of **1** are listed in

Table 1. Crystal data and structure refinement of compound **1**.

Molecular formula	$C_6H_7DyO_8$
Formula weight	369.59
T / K	293(2)
λ / Å	0.71073
Space group	$C2/c$
Crystal system	monoclinic
a / Å	19.145(4)
b / Å	6.0758(12)
c / Å	15.577(3)
β / °	103.35(3)
V / $Å^3$	1762.9(6)
Z, ρ_c / g cm^{-3}	8, 2.762
μ / mm^{-1}	8.500
F(000)	1360
Reflections collected	8178
Indenpant reflections	2013 (R_{int} = 0.0269)
Data/restraints/parameters	2013/0/136
Goodness-of-fit on F_2	1.282
Final R indices $[I > 2\sigma(I)]$[a]	R_1 = 0.0192, wR_2 = 0.0507
R indices (all data)[a]	R_1 = 0.0207, wR_2 = 0.0511

[a] $R_1 = \Sigma||F_o| - |F_c||/\Sigma|F_o|$; $wR_2 = \Sigma[w(F_o^2 - F_c^2)^2]/\Sigma[w(F_o^2)^2]^{1/2}$.

Table 2. CCDC-602711 contains the supplementary crystallographic data for this paper. These data can be obtained free of charge from The Cambridge Crystallographic Data Centre via www.ccdc.cam.ac.uk/data_request/cif.

Table 2. Selected bond lengths [Å] and bond angles [°].

Dy(1)–O(3)	2.321(2)
Dy(1)–O(6)	2.322(3)
Dy(1)–O(5)	2.354(2)
Dy(1)–O(7)#1[a]	2.369(2)
Dy(1)–O(8)	2.425(3)
Dy(1)–O(4)	2.449(3)
Dy(1)–O(7)	2.474(3)
Dy(1)–O(1)	2.489(3)
Dy(1)–O(2)	2.608(3)
O(3)–Dy(1)–O(5)	138.48(9)
O(3)–Dy(1)–O(6)	143.86(10)
O(3)–Dy(1)–O(7)#1[a]	76.55(10)
O(3)–Dy(1)–O(1)	65.86(9)

[a] Symmetry transformations used to generate equivalent atoms: #1 –x, y, $–z + 1/2$.

Supporting Information (see footnote on the first page of this article): Figures of the structure of **1** and magnetic data of **1**.

Acknowledgments

The authors are thankful for the financial support of the National Natural Science Foundation of China (Grant No. 20371010; 20671017) and the Specialized Research Fund for the Doctoral Program of Higher Education.

[1] a) For recent reviews, see: P. J. Hagrman, D. Hagrman, J. Zubieta, *Angew. Chem. Int. Ed.* **1999**, *111*, 2798–2848; b) O. M. Yahgi, M. O'Keeffe, N. W. Ockwig, H. K. Chae, M. Eddaoudi, J. Kim, *Nature* **2003**, *423*, 705–714; c) C. N. R. Rao, S. Natarajan, R. Vaidhyanathan, *Angew. Chem. Int. Ed.* **2004**, *43*, 1466–1496; d) D. Maspoch, D. Ruiz-Molina, J. Veciana, *J. Mater. Chem.* **2004**, *14*, 2713–2723; e) C. Janiak, *Dalton Trans.* **2003**, 2781–2804.

[2] a) For examples, see: S. Golhen, L. Quahab, D. Drandjean, P. Molinie, *Inorg. Chem.* **1998**, *37*, 1499; b) Q. Ye, Y. H. Li, Y. M. Song, X. F. Huang, R. G. Xiong, Z. Xue, *Inorg. Chem.* **2005**, *44*, 3618–3622; c) S. Hermes, M. K. Schröter, R. Schmid, L. Khodeir, M. Muhler, A. Tissler, R. W. Fischer, R. A. Fischer, *Angew. Chem. Int. Ed.* **2005**, *44*, 6237–6241; d) J. P. Costes, F. Dahan, F. Nicodeme, *Inorg. Chem.* **2001**, *40*, 5285–5287; e) S. S. Kaye, J. R. Long, *J. Am. Chem. Soc.* **2005**, *127*, 6506–6507; f) L. Pan, H. Liu, X. Lei, X. Huang, D. H. Olson, N. J. Turro, J. Li, *Angew. Chem. Int. Ed.* **2003**, *42*, 542–546; g) B. Q. Ma, H. L. Sun, S. Gao, *Chem. Commun.* **2003**, 2164–2165.

[3] a) H. Ohno, *Science* **2001**, *291*, 840–841; b) S. A. Wolf, D. D. Awschalom, R. A. Buhrman, J. M. Daughton, S. Molnar, M. L. Roukes, A. Y. Chtchelkanova, D. M. Treger, *Science* **2001**, *294*, 1488–1495; c) J. J. Attema, G. A. de Wijs, G. R. Blake, R. A. de Groot, *J. Am. Chem. Soc.* **2005**, *127*, 16325–16328.

[4] a) R. Sessoli, H. L. Tsai, A. R. Schake, S. Sheyi, J. B. Vincent, K. Folting, D. Gatteschi, G. Christou, D. N. Hendrickson, *J. Am. Chem. Soc.* **1993**, *115*, 1804–1816; b) A. Caneschi, D. Gatteschi, R. Sessoli, A.-L. Barra, L. C. Brunel, M. Guillot, *J. Am. Chem. Soc.* **1991**, *113*, 5873–5874; c) R. Sessoli, D. Gatteschi, A. Caneschi, M. A. Novak, *Nature* **1993**, *365*, 141–143.

[5] a) M. Murrie, H. Stoeckli-Evans, H. U. Güdel, *Angew. Chem. Int. Ed.* **2001**, *40*, 1957–1960; b) M. Murrie, D. Biner, H. Stoeckli-Evans, H. U. Güdel, *Chem. Commun.* **2003**, 230–231; c) S. T. Ochsenbein, M. Murrie, E. Rusanov, H. Stoeckli-Evans, C. Sekine, H. U. Güdel, *Inorg. Chem.* **2002**, *41*, 5133–5140; d) M. Murrie, S. J. Teat, H. Stoeckli-Evans, H. U. Güdel, *Angew. Chem. Int. Ed.* **2003**, *42*, 4653–4656.

[6] S. C. Xiang, X. T. Wu, J. J. Zhang, R. B. Fu, S. M. Hu, X. D. Zhang, *J. Am. Chem. Soc.* **2005**, *127*, 16352–16353.

[7] A. Bino, I. Shweky, S. Cohen, E. R. Bauminger, S. J. Lippard, *Inorg. Chem.* **1998**, *37*, 5168–5172.

[8] I. Gautier-Luneau, C. Fouquard, C. Merle, J. L. Pierre, D. Luneau, *J. Chem. Soc. Dalton Trans.* **2001**, 2127–2131.

[9] Z. H. Zhou, Y. F. Deng, Z. X. Cao, R. H. Zhang, Y. L. Chow, *Inorg. Chem.* **2005**, *44*, 6912–6914.

[10] Z. H. Zhou, Y. F. Deng, H. L. Wan, *Cryst. Growth Des.* **2005**, *5*, 1109–1117.

[11] N. Kotsakis, C. P. Raptopoulou, V. Tangoulis, A. Terzis, J. Giapintzakis, T. Jakusch, T. Kiss, A. Salifoglou, *Inorg. Chem.* **2003**, *42*, 22–31.

[12] a) R. Baggio, M. Perec, *Inorg. Chem.* **2004**, *43*, 6965–6968; b) Y. Q. Yuan, Y. Q. Xu, M. Y. Wu, M. C. Hong, *Acta Crystallogr., Sect. E* **2005**, *61*, m108–m109; c) S. G. Liu, W. Liu, J. L. Zuo, Y. Z. Li, X. Z. You, *Inorg. Chem. Commun.* **2005**, *8*, 328–330; d) R. Baggio, R. Calvo, M. T. Garland, O. Peña, M. Perec, A. Rizzi, *Inorg. Chem.* **2005**, *44*, 8979–8987.

[13] a) J. Tang, I. Hewitt, N. T. Madhu, G. Chastanet, W. Wernsdorfer, C. E. Anson, C. Benelli, R. Sessoli, A. K. Powell, *Angew. Chem. Int. Ed.* **2006**, *45*, 1729–1733; b) C. M. Zaleski, E. C. Depperman, J. W. Kampf, M. L. Kirk, V. L. Pecoraro, *Angew. Chem. Int. Ed.* **2004**, *43*, 3912–3914; c) A. Mishra, W. Wernsdorfer, K. A. Abboud, G. Christou, *J. Am. Chem. Soc.* **2004**, *126*, 15648–15649.

[14] a) H. W. Hou, G. Li, L. K. Li, Y. Zhu, X. R. Meng, Y. T. Fan, *Inorg. Chem.* **2003**, *42*, 428–435; b) J. A. Mydosh, *Spin Glasses: An Experimental Introduction*, Taylor and Francis, London, **1993**.

[15] O. Daisuke, M. Takeshi, N. Hironori, M. Youichi, *J. Phys. Soc. Jpn.* **2005**, *74*, 2434–2437.

[16] a) S. Gao, G. Su, T. Yi, B. Q. Ma, *Phys. Rev. B* **2001**, *63*, 054431; b) B. Q. Ma, S. Gao, G. Su, G. X. Xu, *Angew. Chem. Int. Ed.* **2001**, *40*, 434–437; c) Q. D. Liu, J. R. Li, S. Gao, B. Q. Ma, Q. Z. Zhou, K. B. Yu, H. Liu, *Chem. Commun.* **2000**, 1685–1686; d) Y. Z. Zhang, G. P. Duan, O. Sato, S. Gao, *Dalton Trans.* **2006**, 2625–2634.

Received: November 25, 2006
Published Online: June 5, 2007

